



Gazi University

Journal of Science

PART A: ENGINEERING AND INNOVATION

<http://dergipark.org.tr/guj.1247152>

Self-Powered Mechanical Energy Sensor Application of SnO₂/Ag and PMMA/ITO Nanocomposites via Triboelectric Effect

Gizem DURAK YÜZÜAK¹ Mehmet ÇETİN² Ercüment YÜZÜAK^{2*}

¹Munzur University, Rare Earth Elements Application and Research Center, Tunceli, Türkiye

²Recep Tayyip Erdoğan University, Faculty of Engineering and Architecture, Rize, Türkiye

Keywords	Abstract
Triboelectric Nanotechnology Nano-Energy Self-Electric Contact Dedector (SPCS)	The triboelectric nanogenerator is a state-of-the-art device for addressing the growing problem of meeting the world's ever-increasing energy needs by converting mechanical energy into electrical energy. Using the popular semiconductor SnO ₂ nanostructured thin films as a triboelectric layer over contact regions, as opposed to polymers with lesser performance, increases the output power and life time of nanogenerators. In order to design a triboelectric nanogenerator, deposited thin film SnO ₂ is used as a friction layer with Ag electrode after heat-treatment at 623 K with a contrary layer of PMMA poly (methyl-methacrylate) with ITO electrode. The structural and electrical properties were analyzed by using scanning electron microscopy (SEM), electro-impedance spectroscopy (EIS) and atomic force microscopy (AFM) measurements. The increased output power of the triboelectric nanogenerator is attributed to the nanoscale PMMA contact charge created by tunneling electrons in the SnO ₂ /Ag nanocomposite thin film layer. Due to its proximity to the PMMA/ITO surface, the SnO ₂ /Ag layer causes electron field emission, and tapping the SnO ₂ /Ag layer may result in electron cloud overlap. Similar to a semiconductor/insulator interface, the Fermi level of SnO ₂ plays a crucial role in electron transport. The system efficiency stated as a touch detector in a conventional keyboard that generates its own power is revealed in part by an analysis of its operating state up to the 4V.

Cite

Yüzüak, G. D., Çetin, M., & Yüzüak, E. (2023). Self-Powered Mechanical Energy Sensor Application of SnO₂/Ag and PMMA/ITO Nanocomposites Via Triboelectric Effect. *GU J Sci, Part A, 10(2)*, 149-156. doi:10.54287/guj.1247152

Author ID (ORCID Number)	Article Process
0000-0002-2358-8789	Gizem DURAK YÜZÜAK
0000-0001-6422-4634	Mehmet ÇETİN
0000-0002-2521-9362	Ercüment YÜZÜAK
	Submission Date 03.02.2023
	Revision Date 27.03.2023
	Accepted Date 03.04.2023
	Published Date 12.06.2023

1. INTRODUCTION

Scientists have been conducting a variety of studies for years in an effort to find a solution to the world's energy dilemma by uncovering new forms of energy. One of the current issues in renewable and clean-energy generation is the development of new methods that can compare various energy sources. Artificial forces, including wind and rain (also known as variable forces), or other forces resulting from human activities have the characteristics of being waste and may be recovered to provide electricity (Xia et al., 2019). The triboelectric effect (TEE) is a natural phenomenon that facilitates the design of simple and cheap devices for transforming mechanical energy into electrical power (Wang, 2020). Through the frictional charging method, mechanical energy may be converted into electrical power, allowing for the operation of tiny electronic devices within the context of a low-cost, straightforward, and efficient strategy via the triboelectric nanogenerator (TENG). A surface charge is generated at the interface between two dissimilar dielectrics. As the separation between the two dielectrics grows, so does the rate at which electrons may move from one electrode to the other. Originally, TENGs have had electrodes connected to both the above and bottom sides of two dissimilar layers that face each other (Wang, 2020). The triboelectric effect is its primary mechanism for accomplishing this purpose. On the basis of this working feature, TENGs are used

*Corresponding Author, e-mail: ercument.yuzuak@erdogan.edu.tr

as: a) mechanical energy harvesting structure from the vibration source as a form of mechanical energy capture devices (Chen & Wang, 2017), b) self-powered sensors (Tasneem et al., 2022), c) wave energy harvesters (Liang et al., 2023), d) biomechanical energy harvesters acting as power sources for other electronic devices (Babu et al., 2022).

The rapid advancement and increasing popularity of portable and handheld chemical or biosensors in recent decades has posed a scientific issue for their sustained energizing. Therefore, mechanical energy harvesters have lately been investigated, either as detectors or threshers to retain charge in compact, long-lasting energy-storage devices to power the detectors (Khandelwal & Dahiya, 2022; Zheng et al., 2022). Examples of such harvesters include piezoelectric and triboelectric generators (TEGs). With such multifunctional actions, fewer instruments are required in a system, which allows to address the technical challenges; this is especially intriguing when it comes to the usage of energy harvesters as detectors. While evidence of the triboelectric effect dates to antiquity, the precise mechanism by which it works remains a matter of intense debate. Many different processes, including electron transfer, ion transfer, bond dissociation, chemical change, and material transfer, may be at play depending on the specific material and ambient conditions (Wang & Wang 2019; Wang, 2015). Triboelectric nanogenerators (TENGs) are electrical circuit-forming devices made from the coupling of layers with dissimilar properties by the use of complementary conductors (Zhu et al., 2015). Given their low cost and ease of manufacture, polymers can be found in almost every modern technological device. These structures are often used in triboelectric systems; however, they are readily distorted after prolonged usage. However, semiconductor thin films provide an alternative to polymers because of their extended service lives, resistance to harsh environments, and ability to be created with a surface roughness on the nanoscale, depending on the application (Yüzüak et al., 2022). While applied to the structure, mechanical deformation occurs when creating parallel but opposing loads on the surfaces. Depending on the instantaneous potential shift, the supplied electron flow facilitates the creation of power that is needed by tiny electronic devices. Nanogenerators are a promising new technology for addressing the growing challenge of meeting the world's ever-increasing energy needs. Increasing the surface charge density is important to boost the triboelectric effect's effectiveness (Wang & Wang, 2019). This may be achieved by adjusting the micro- and nanostructures as well as the effective contact surface area. For example, several research projects have sought to produce polymer surfaces as electrodes in TENGs. Although polymers are simple to be manufactured, they fall short in performance because of how quickly they distort under stress. The most crucial factor in improving TENG's efficiency is ensuring long-term performance and switching to electrode materials with a higher rate of electron loss compared to polymers. Compared to TiO_2 or ZnO , the n-type semiconductor SnO_2 is an attractive option because of its carrier mobility ($100\text{-}200\text{ cm}^2/\text{V}\cdot\text{s}$) (Breckenridge & Hosler, 1953) and broad band gap (3.62 eV), both of which point to a more rapid transit of photo-generated electrons and better long-term electron stability (Gao et al., 2014). In addition, when other materials, such as TiO_2 or ZnO , are used, a surface dipole layer is formed toward SnO_2 due to its low net charge and positive charge transfer boundary (G. Yang et al., 2012).

The research conducted by the reference (N. H. Lee et al., 2017) is one of the most impressive outcomes found for this semiconductor in the published paper. Based on the research presented in the paper, a semiconductor SnO_2 triboelectric layer may be created by placing an Al-coated electrode on a Pt substrate. After determining that this was not enough, the researchers attempted to cover the electrode's AlO_2 substrate to boost its efficiency. But there are difficulties in the manufacturing procedure. The electrodes made using ALD required an additional annealing step since the first heating and cooling cycles did not result in the expected crystallization. The result is a delay in the manufacturing process. Pt coating is an extra and very costly feature. When they realized there was a glitch in the experiment, they added Al_2O_3 beneath the SnO_2 to boost its conductivity. A similar Al electrode was utilized. The resulting thin films have a thickness of 5-25 nm. The results of this analysis reveal: a voltage of 125 V, a current density of $2.75\text{ A}/\text{cm}^2$, and a power density of $0.344\% \text{ mW}/\text{cm}^2$. Other research has shown that heating SnO_2 films to temperatures between 773 K and 1073 K results in a tetragonal structure (Terrier et al., 1997). It was found that the thin film with the substrate was heated to 473 K, and SnO_2 films developed in a tetragonal crystal structure (Wang, 2013). The tetragonal structure is known to have a greater charge density all around the density of state in the vicinity of Fermi energy.

In the present work, thin films with semiconductor features will be used as a triboelectric layer on the friction surface, with the expectation that this will improve efficiency. It is hypothesized that the created TENG will profit more from using a SnO₂ layer, as semiconductors have the property of delivering long-term performance and losing electrons quicker than polymers. For this aim,

- The Ag electrode and SnO₂ thin films generated on the Si(100) substrate using the magnetron sputtering technique and,
- The PMMA/ITO structure is what will be used to create the secondary electrode component

was used to form of the TENG. After doing characterizations to the friction layer, the potential changes in the electrical output power of the TENGs will be explored, by using a contact sensor in a commercial computer keyboard that generates its own energy and has been proven to have this efficiency.

2. MATERIAL AND METHOD

Conventional RF and DC magnetron co-sputtering were used to deposit SnO₂ and Ag layers onto Si(100) substrates. For the sputtering process, a SnO₂ target (99.999%) with dimensions of 2 inches in diameter and 0.250 inches in thickness was used in a high-vacuum chamber with a pressure of more than 2×10^{-6} Torr. Argon and oxygen inert gases (6N) were used at a working pressure of 5 mTorr. To keep the film consistent throughout its thickness, we rotated the substrate at 12 rpm as it was growing up. SnO₂ films' high-temperature crystal phase effect on Ag buffer via 673 K heat-treatment was investigated by scanning electron microscopy (SEM) with energy dispersive X-ray (EDX), atomic force microscopy (AFM), and electro-impedance spectroscopy measurements (EIS) for structural and electrical characterizations.

TENG is formed by combining these two different parts of electrodes with electrical connections (Figure 1a) and its working mechanism representation in contact separation mode (Figure 1b). The potential changes in the contact density of the semiconductor thin film and the electrical output power of TENG will be examined due to the different physical properties and different surface roughness of the SnO₂ thin films used in the produced TENGs. For better performance, the SnO₂ thin films are heat-treated at 673 K. For the purpose of applying consistent external forces, we used an analogue oscilloscope to coordinate the timing of the pushing motion and a force indicator to regulate the pushing forces themselves. As the second friction electrode, PMMA/ITO film was considered because of its strong negative force, simplicity of production, and basic approach. The effective surface area of TENGs was about 0.32 cm². No fluctuations were found, and; all readings were taken under constant circumstances. We used a four-channel digital storage oscilloscope and a DC 24 V, 10-100 rpm mechanic motor coupled to a linear gear to measure the resulting electrical output. As a result of connecting the oscilloscope's two terminals, the open circuit voltage (V_{OC}) was calculated over ITO and Ag electrodes. All measurements of electrical performance were carried out at room temperature with a relative humidity of 55% RH. The holding cell for EIS measurements was protected by a grounded shield.

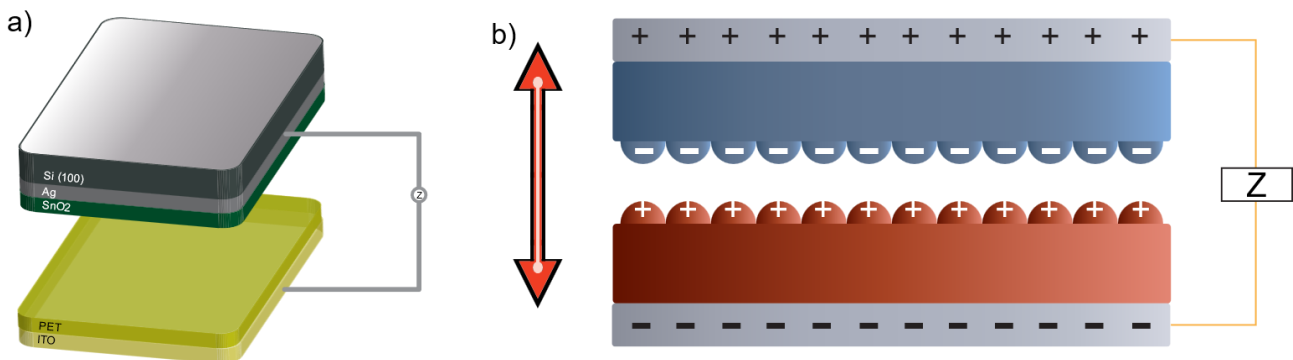


Figure 1. a) Layers in TENG in the present study and b) its working mechanism representation on contact separation mode

3. RESULTS AND DISCUSSION

SEM pictures of the surface morphology of the untreated and 673 K SnO₂ thin films are shown in Figures 2a and 2b in a systematic manner. Based on electron microscopy micrographs as seen in Figure 2a and 2b, it was found that heat treatment altered the surface morphology irreversibly. Tiny grains make up the unprocessed sample. There are agglomerates formed when grains are linked together. The surface morphology of SnO₂ film is unaltered by annealing to 673 K, and it has the same film-like appearance. From the result obtained, it is seen in Figure 2a that the untreated thin film produced at 50 Watt of sputtering power and 5 mTorr of sputtering pressure with a thickness of 200 nm is homogeneously deposited on the surface and has a spherical particle structure. A heat treatment at 673 K was found to have no effect on the particle size of the thin film compared to its pre-heat-treatment enlargement condition.

On the surface of the thin film, however, aggregation was shown to have risen. The SnO₂ films that were formed at high temperatures were discovered to have cracks as well as macroscopic flaws, as it was reported in the research that was published (Turan et al., 2022). It was observed to be free from macroscopic defects. Coating islands might originate from the unwinding of tensile stress on the film coat or from the removal and ignition of phase transition after continuous heat treatment (Zakaria et al., 2022). Using the EDX, we were able to determine the chemical content and purity of SnO₂ thin films that had been formed at room temperature. According to the EDX results, within the experimental error, the atomic percentage of elements Sn and O in the SnO₂ thin film formed was found to be in close agreement with the nominal stoichiometry.

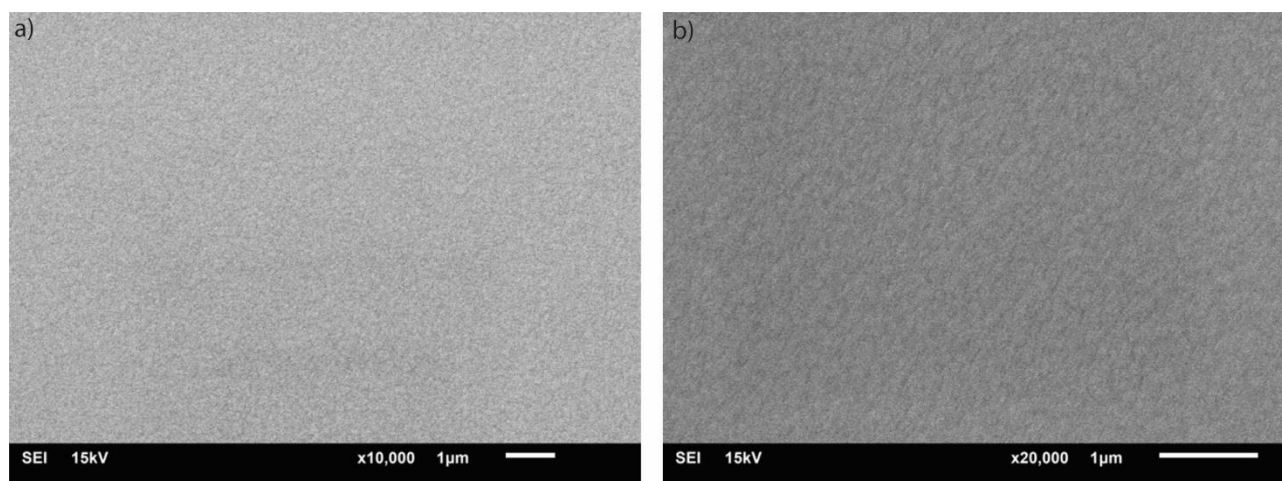


Figure 2. SEM micrographs of a) untreated and b) 673 K thin films

EIS was used to evaluate the electrochemical characteristics of thin films. Figures 3a and 3b depict, in the range of 1V–2.2V bias voltages, the frequency-dependent real (Z_1, Z') and imaginary (Z_2, Z'') impedance part plots (Nyquist plots) of the as-deposited SnO₂ and 673 K thin films. EIS spectrum analyzer was used to model the electrochemical impedance behavior by means of the corresponding electrical circuit (inset of Figure 3a) (Bondarenko & Ragoisha, 2005). The resistance of the solution and all its associated contacts made up "R_s" in the circuit, whereas "R_p" represented the charge transfer resistance. A material's electrical properties can be seen in the form of semicircular arcs. The illustration clearly depicts a single semicircle, but another study observed two semicircles in SnO₂ film (Chandra Bose et al., 2005). Understanding the mechanism and processes of electron transport can be aided by the EIS (Ouyang et al., 2014). Plots show that the hopping phenomenon in semiconductors causes the real part (Z') impedance to rise with decreasing frequency. Accumulated charge carriers at the grain boundaries have enough energy to hop the barrier at low frequencies, which is great for operating at the TENGs' intrinsically low oscillation frequency. This circumstance is reminiscent of one's seen in earlier research, and the dissipation rate of conductivity is measured in terms of its "hopping frequency" (Shen et al., 2018). The actual component of the complex impedance, as measured by comparing two plots, decreases with increasing frequency, a trend that correlates with the particles' grain boundaries. The whole thin film frequency changes upward as particle size grows.

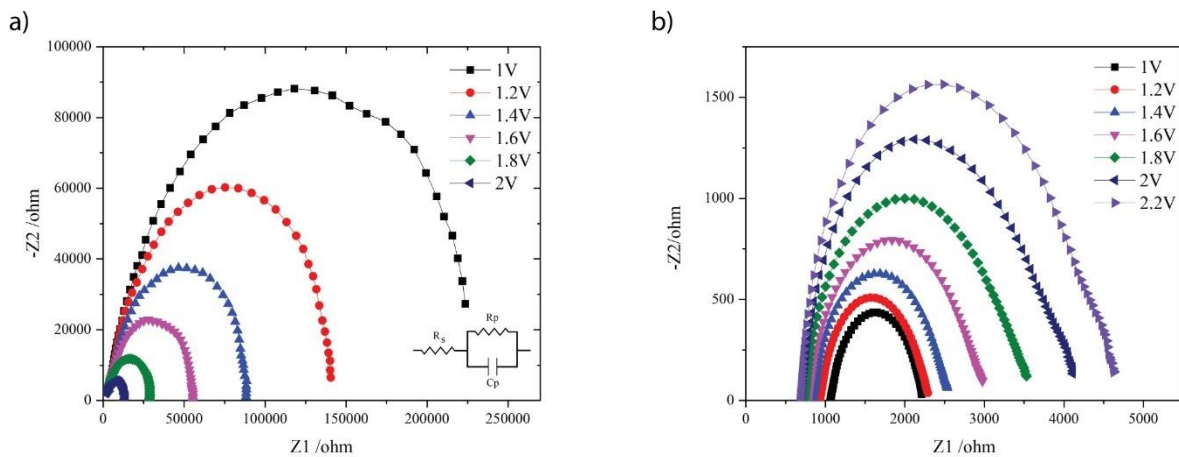


Figure 3. EIS measurements of **a)** untreated and **b)** 673 K thin films

Atomic force microscopy, used in non-contact mode, was employed to examine the SnO₂ film's surface topography. Here, the probe cantilever's frequency is oscillated very close to its natural resonance. Figures 4a, 4b, 4c and 4d, 4e, 4f reveal AFM images and line height analysis of untreated and 673 K treated thin films, respectively. AFM images (2D and 3D) were produced, which also bolstered the surface roughness investigations that were performed subsequently. These AFM images demonstrated that post-heat treatment surface roughness was much higher. The results are generally consistent with those of earlier investigations, with some small variations (Muthukrishnan et al., 2022). It is believed to be the result of microscopic and nanoscale flaws in the crystal structure produced between the semiconductor and conductive layers. The images clearly show that the surface morphology of the 100 nm thin film comprises spherical particles. This can be noticed when looking at the images. It can be noted that the findings obtained are consistent with those acquired using SEM.

The linear facial profile measurements acquired with the AFM were also very helpful. Figures 4b and 4e illustrate the results before and after heat treatment, respectively. It appears to have had a dramatic change in its development between before and after heat treatment, as measured by the depth of its surface, as shown by these numbers. According to this, the depths were shallow (-9 μm to 7 μm) before the heat treatment but grew significantly (-15 μm to 11 μm) thereafter. We can attribute this to the fact that Sn and O₂ ratios have levelled out on a regional scale (J. R. Lee et al., 2007). The surface roughness plots generated have about the value of 1.7 nm and 5.2 nm as its average value for untreated and 673 K, respectively. This result is consistent with the literature that we have reviewed, which supports our results (Y. Yang et al., 2022). The topographical image may be used to produce a 3D image, which can then be used to study the particles' distribution, which can be seen to be uniform.

In terms of applicability, we implemented TENG in a traditional keyboard designed for usage on desktop computers in the office. Using double-sided conductive silver tape, the SnO₂/Ag - PMMA/ITO film composite developed in this work was attached to the secured beneath the "Enter" key of a commercial keyboard. The findings for the scenario with the help of a digital oscilloscope are shown in Figure 5a. With the use of the enter key and a raised hand, we were able to get an output voltage of up to 2 V. The continuous pressing and releasing action, on the other hand, results in a maximum of 4 V but exhibits some discontinuity, as seen in Figure 5b. Pulses obtained at low frequencies were much more stable than those obtained by increasing the key press speed. This situation can be considered an output of triboelectric technology, which is both reactive and a function of frequency. The variance in force used to push the enter key is regarded as the primary cause of this break in continuity. So, it is safe to assume that the next generation of sensing and self-powered smart keycap technology will be ushered in by the logical processing of these electrical pulses.

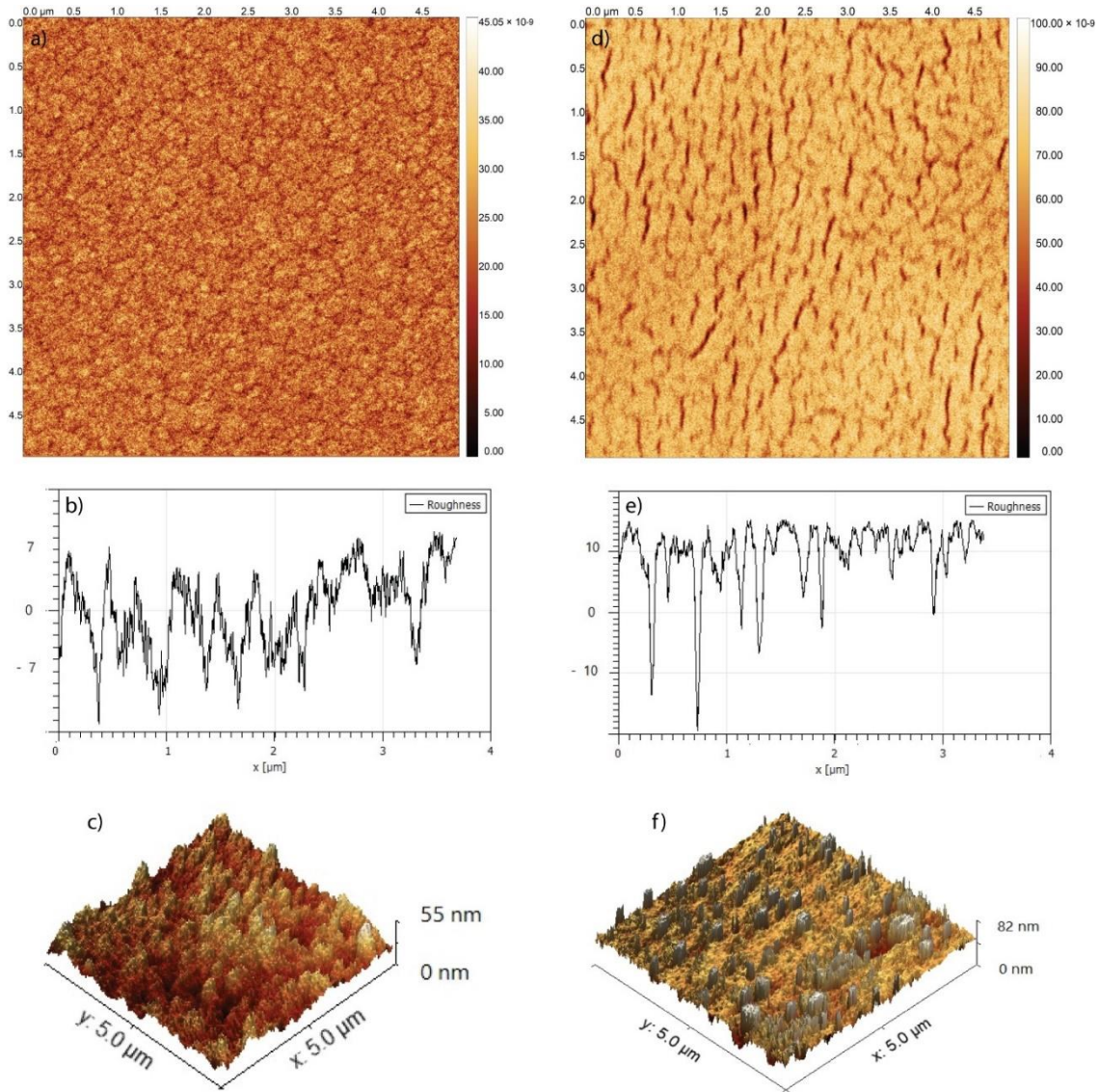


Figure 4. 2D, line profiles and 3D AFM measurements of *a), b), c)* untreated and *d), e), f)* 673 K thin films, respectively

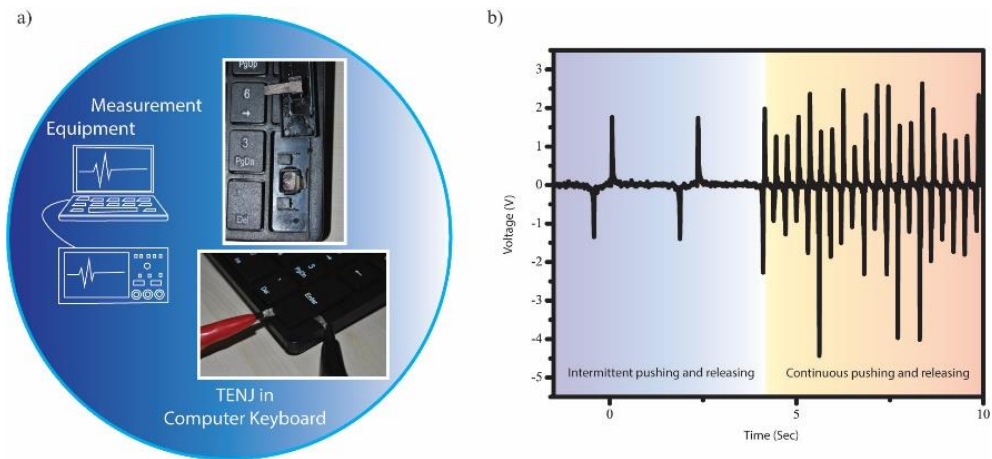


Figure 5. *a)* Triboelectric nanogenerator and measuring mechanism mounted on the mechanical keyboard, *b)* electrical voltage measurement graphs obtained with this mechanism in periods I (intermittent pressing and releasing) and II (continuous pressing and releasing)

4. CONCLUSION

Triboelectric systems are newly presented renewable and clean energy sources worldwide. The discovery of new systems with triboelectric properties and the use of these systems in electricity generation technology are of great importance, both technologically and in terms of existing science and literature. In this study, the improvement was achieved only by the deposition of SnO₂ thin films with an Ag buffer layer on the Si (100) substrate, without any sublayer or electrical poling. In order to make the work visible and applicable, the keyboard application was tried as a prototype of a physical application of this. It is apparent that the use of semiconductors in this kind of application area will lead to a rise in the number of places where they are put to be used. Therefore, the study presented here will provide a novel outlook on boosting triboelectric effect features.

ACKNOWLEDGEMENT

This work was supported by the Scientific and Technological Research Council of Turkey (TÜBİTAK) under the grant number of 119M972. The research for the present work was carried out by the Functional Materials Research Group (FMRG) at Recep Tayyip Erdogan University. Some parts of the study were presented at the 9th International Conference on Materials Science and Nanotechnology for Next Generation (MSNG-2022).

CONFLICT OF INTEREST

The authors declare no conflict of interest.

REFERENCES

- Babu, A., Rakesh, D. Supraja, P., Mishra, S., Kumar, K. U., Kumar, R. R., Haranath, D., Mamidala, E., & Nagapuri, R. (2022). Plant-based triboelectric nanogenerator for biomechanical energy harvesting. *Results in Surfaces and Interfaces*, 8, 100075. doi:[10.1016/j.rsurfi.2022.100075](https://doi.org/10.1016/j.rsurfi.2022.100075)
- Breckenridge, R. G., & Hosler, W. R. (1953). Electrical properties of titanium dioxide semiconductors. *Physical Review*, 91(4), 793-802. doi:[10.1103/PhysRev.91.793](https://doi.org/10.1103/PhysRev.91.793)
- Bondarenko, A. S., & Ragoisha, G. A. (2005). EIS Spectrum Analyser. In: Pomerantsev A. L. (Eds.), *Progress in Chemometrics Research* (pp. 89-102). Nova Science Publishers: New York. [URL](#)
- Chandra Bose, A., Thangadurai, P., Ramasamy, S., & Purniah, B. (2005). Impedance spectroscopy and DSC studies on nanostructured SnO₂. *Vacuum*, 77(3), 293-300. doi:[10.1016/j.vacuum.2004.10.007](https://doi.org/10.1016/j.vacuum.2004.10.007)
- Chen, J., & Wang, Z. L. (2017). Reviving Vibration Energy Harvesting and Self-Powered Sensing by a Triboelectric Nanogenerator. *Joule*, 1(3), 480-521. doi:[10.1016/j.joule.2017.09.004](https://doi.org/10.1016/j.joule.2017.09.004)
- Gao, C., Li, X., Zhu, X., Chen, L., Zhang, Z., Wang, Y., Zhang, Z., Duan, H., & Xie, E. (2014). Branched hierarchical photoanode of titanium dioxide nanoneedles on tin dioxide nanofiber network for high performance dye-sensitized solar cells. *Journal of Power Sources*, 264, 15-21. doi:[10.1016/j.jpowsour.2014.04.059](https://doi.org/10.1016/j.jpowsour.2014.04.059)
- Khandelwal, G., & Dahiya R. (2022). Self-powered active sensing based on triboelectric generator, *Advanced Materials*, 34(33), 2200724. doi:[10.1002/adma.202200724](https://doi.org/10.1002/adma.202200724)
- Lee, N. H., Yoon, S. Y., Kim, D. H., Kim, S. K., & Choi, B. J. (2017). Triboelectric Charge Generation by Semiconducting SnO₂ Film Grown by Atomic Layer Deposition. *Electronic Materials Letters*, 13(4), 318-323. doi:[10.1007/s13391-017-6289-0](https://doi.org/10.1007/s13391-017-6289-0)
- Lee, J. R., Kim, D. G., Lee, G. H., Park, Y. H., & Song, P. K. (2007). Characteristics of IZSO films deposited by a co-sputtering system. *Metals and Materials International*, 13(5), 399-402. doi:[10.1007/BF03027875](https://doi.org/10.1007/BF03027875)

- Liang, X., Liu, S., Yang, H., & Jiang, T. (2023). Triboelectric Nanogenerators for Ocean Wave Energy Harvesting: Unit Integration and Network Construction. *Electronics*, 12(1), 225. doi:[10.3390/electronics12010225](https://doi.org/10.3390/electronics12010225)
- Muthukrishnan, A. P., Lee, J., Kim, J., Kim, C. S., & Jo, S., (2022). Low-temperature solution-processed SnO₂ electron transport layer modified by oxygen plasma for planar perovskite solar cells. *RSC Advances*, 12(8), 4883-4890. doi:[10.1039/D1RA08946C](https://doi.org/10.1039/D1RA08946C)
- Shen, W., Ou, T., Wang, J., Qin, T., Zhang, G., Zhang, X., Han, Y., Ma, Y., & Gao, C. (2018). Effects of high pressure on the electrical resistivity and dielectric properties of nanocrystalline SnO₂. *Scientific Reports*, 8, 5086. doi:[10.1038/s41598-018-22965-8](https://doi.org/10.1038/s41598-018-22965-8)
- Tasneem, N. T., Biswas, D. K., Adhikari, P. R., Gunti, A., Patwary, A. B., Reid, R. C., & Mahbub, I. (2022). A self-powered wireless motion sensor based on a high-surface area reverse electrowetting-on-dielectric energy harvester. *Scientific Reports*, 12, 3782. doi:[10.1038/s41598-022-07631-4](https://doi.org/10.1038/s41598-022-07631-4)
- Terrier, C., Chatelon, J. P., & Roger, J. A. (1997). Electrical and optical properties of Sb:SnO₂ thin films obtained by the sol-gel method. *Thin Solid Films*, 295(1-2), 95-100. doi:[10.1016/S0040-6090\(96\)09324-8](https://doi.org/10.1016/S0040-6090(96)09324-8)
- Turan, E., Kul, M., & Akin, S. (2022). Structural and optical investigation of spray-deposited SnO₂ thin films. *Journal of Materials Science: Materials in Electronics*, 33(19), 15689-15703. doi:[10.1007/s10854-022-08472-7](https://doi.org/10.1007/s10854-022-08472-7)
- Ouyang, P., Zhang, H., Wang, Y., Chen, W., & Li, Z. (2014). Electrochemical & microstructural investigations of magnetron sputtered nanostructured ATO thin films for application in Li-ion battery. *Electrochimica Acta*, 130, 232-238. doi:[10.1016/j.electacta.2014.03.021](https://doi.org/10.1016/j.electacta.2014.03.021)
- Wang, Z. L. (2013). Triboelectric Nanogenerators as New Energy Technology for Self-Powered Systems and as Active Mechanical and Chemical Sensors. *ACS Nano*, 7(11), 9533-9557. doi:[10.1021/nn404614z](https://doi.org/10.1021/nn404614z)
- Wang, Z. L. (2015). Triboelectric nanogenerators as new energy technology and self-powered sensors-Principles, problems and perspectives. *Faraday Discussions*, 176, 447-458. doi:[10.1039/C4FD00159A](https://doi.org/10.1039/C4FD00159A)
- Wang, Z. L. (2020). On the first principle theory of nanogenerators from Maxwell's equations. *Nano Energy*, 68, 104272. doi:[10.1016/j.nanoen.2019.104272](https://doi.org/10.1016/j.nanoen.2019.104272)
- Wang, Z. L., & Wang, A. C. (2019). On the origin of contact-electrification. *Materials Today*, 30, 34-51. doi:[10.1016/j.mattod.2019.05.016](https://doi.org/10.1016/j.mattod.2019.05.016)
- Xia, X., Fu, J., & Zi, Y. (2019). A universal standardized method for output capability assessment of nanogenerators. *Nature Communications*, 10, 4428. doi:[10.1038/s41467-019-12465-2](https://doi.org/10.1038/s41467-019-12465-2)
- Yang, G., Yan, Z., & Xiao, T. (2012). Preparation and characterization of SnO₂/ZnO/TiO₂ composite semiconductor with enhanced photocatalytic activity. *Applied Surface Science*, 258(22), 8704-8712. doi:[10.1016/j.apsusc.2012.05.078](https://doi.org/10.1016/j.apsusc.2012.05.078)
- Yang, Y., Maeng, B., Jung, D. G., Lee, J., Kim, Y., Kwon, J., An, H. K., & Jung, D. (2022). Annealing Effects on SnO₂ Thin Film for H₂ Gas Sensing. *Nanomaterials*, 12(18), 3227. doi:[10.3390/nano12183227](https://doi.org/10.3390/nano12183227)
- Yüzüak, D. G., Karagöz, C., & Yüzüak, E. (2022). Exploring the Sputtering Conditions in ZnO Thin Film for Triboelectric Nanogenerator Electrode. *International Journal of Energy Research*, 46(14), 20494-20500. doi:[10.1002/er.7777](https://doi.org/10.1002/er.7777)
- Zakaria, Y., Aïssa, B., Fix, T., Ahzi, S., Samara, A., Mansour, S., & Slaoui, A. (2022). Study of wide bandgap SnOx thin films grown by a reactive magnetron sputtering via a two-step method. *Scientific Reports*, 12(1), 15294. doi:[10.1038/s41598-022-19270-w](https://doi.org/10.1038/s41598-022-19270-w)
- Zheng, Y., Liu, T., Wu, J., Xu, T., Wang, X., Han, X., Cui, H., Xu, X., Pan, C., & Li, X. (2022). Energy conversion analysis of multi-layered triboelectric nanogenerators for synergistic rain and solar energy harvesting. *Advanced Materials*, 34(28), 2202238. doi:[10.1002/adma.202202238](https://doi.org/10.1002/adma.202202238)
- Zhu, G., Peng, B., Chen, J., Jing, Q., & Wang, Z. L. (2015). Triboelectric nanogenerators as a new energy technology: From fundamentals, devices, to applications. *Nano Energy*, 14, 126-138. doi:[10.1016/j.nanoen.2014.11.050](https://doi.org/10.1016/j.nanoen.2014.11.050)